

## Research



**Cite this article:** Ducklow HW *et al.* 2018 Spring–summer net community production, new production, particle export and related water column biogeochemical processes in the marginal sea ice zone of the Western Antarctic Peninsula 2012–2014. *Phil. Trans. R. Soc. A* **376**: 20170177.

<http://dx.doi.org/10.1098/rsta.2017.0177>

Accepted: 14 March 2018

One contribution of 14 to a theme issue ‘The marine system of the West Antarctic Peninsula: status and strategy for progress in a region of rapid change’.

### Subject Areas:

oceanography, biogeochemistry

### Keywords:

Antarctica, ocean biogeochemistry, net community production, carbon export, thorium-234 deficiency

### Author for correspondence:

Hugh W. Ducklow

e-mail: [hducklow@ldeo.columbia.edu](mailto:hducklow@ldeo.columbia.edu)

<sup>†</sup>Present address: Department of Earth, Ocean and Atmospheric Science, Florida State University, Tallahassee, FL, USA.

<sup>‡</sup>Present address: Department of Environmental Sciences, University of Virginia, Charlottesville, VA, USA.

<sup>¶</sup>Present address: Department of Chemistry, University of York, Heslington, York, UK.

Electronic supplementary material is available online at <https://doi.org/10.6084/m9.figshare.c.4055849>.

# Spring–summer net community production, new production, particle export and related water column biogeochemical processes in the marginal sea ice zone of the Western Antarctic Peninsula 2012–2014

Hugh W. Ducklow<sup>1</sup>, Michael R. Stukel<sup>1,†</sup>, Rachel Eveleth<sup>2,‡</sup>, Scott C. Doney<sup>3</sup>, Tim Jickells<sup>4</sup>, Oscar Schofield<sup>5</sup>, Alex R. Baker<sup>4</sup>, John Brindle<sup>4</sup>, Rosie Chance<sup>4,¶</sup> and Nicolas Cassar<sup>2</sup>

<sup>1</sup>Lamont-Doherty Earth Observatory, Columbia University, Palisades, NY, USA

<sup>2</sup>Nicholas School of Environment, Duke University, Durham, NC, USA

<sup>3</sup>Department of Environmental Sciences, University of Virginia, Charlottesville, VA, USA

<sup>4</sup>School of Environmental Sciences, University of East Anglia, Norwich, UK

<sup>5</sup>Department of Marine and Coastal Sciences, Rutgers University, New Brunswick, NJ, USA

HWD, 0000-0001-9480-2183; OS, 0000-0003-2359-4131

New production (New P, the rate of net primary production (NPP) supported by exogenously supplied limiting nutrients) and net community production (NCP, gross primary production not consumed by community respiration) are closely related but mechanistically distinct processes. They set the carbon balance in the upper ocean and define an upper limit for export from the system. The relationships, relative magnitudes and variability of New P (from <sup>15</sup>NO<sub>3</sub><sup>-</sup> uptake), O<sub>2</sub>: argon-based NCP and sinking particle export (based on the <sup>238</sup>U: <sup>234</sup>Th disequilibrium) are

increasingly well documented but still not clearly understood. This is especially true in remote regions such as polar marginal ice zones. Here we present a 3-year dataset of simultaneous measurements made at approximately 50 stations along the Western Antarctic Peninsula (WAP) continental shelf in midsummer (January) 2012–2014. Net seasonal-scale changes in water column inventories (0–150 m) of nitrate and iodide were also estimated at the same stations. The average daily rates based on inventory changes exceeded the shorter-term rate measurements. A major uncertainty in the relative magnitude of the inventory estimates is specifying the start of the growing season following sea-ice retreat. New P and NCP(O<sub>2</sub>) did not differ significantly. New P and NCP(O<sub>2</sub>) were significantly greater than sinking particle export from thorium-234. We suggest this is a persistent and systematic imbalance and that other processes such as vertical mixing and advection of suspended particles are important export pathways.

This article is part of the theme issue ‘The marine system of the west Antarctic Peninsula: status and strategy for progress in a region of rapid change’.

## 1. Introduction

The carbon cycles of ecosystems, including the ocean, are driven by the balance between two opposing metabolic processes: gross primary production (GPP) and community respiration (R) (figure 1). The net community production (NCP [1]) defines the nature of that balance between production and destruction of organic matter [1–5]. When  $GPP > R$ , the NCP is positive and the accumulated material is available for export and harvest [6]. At steady state (which most ocean ecosystems approach under most conditions [7]), the rate of new production, i.e. primary production supported by exogenous inputs of a limiting nutrient, approximates the NCP and sets an upper limit for export from the euphotic zone [8]. However, in spite of their frequently observed quantitative similarity, new and net community production are mechanistically distinct processes [9]. As Laws [10] states, it is conceptually and practically difficult to equate the two concepts.

Further hindering understanding of these processes is a lack of comparison of estimates in different systems and over a range of time and space scales [11,12]. Systematic observations in polar, marginal sea-ice zones are particularly poorly represented. Here we present observations of net primary production (NPP) (<sup>14</sup>C), NCP(O<sub>2</sub>), nitrate-based new production and particle export made along the Western Antarctic Peninsula (WAP) in January (midsummer) 2012–2014, along with measurements of physical and biogeochemical properties. These 3 years were selected for analysis because of the availability of <sup>15</sup>NO<sub>3</sub><sup>−</sup> uptake rate estimates of New Production (New P) (2012–2014) and water column iodide accumulation (2012 only), accompanying NPP(<sup>14</sup>C) measurements from <sup>14</sup>C-bicarbonate uptake, oxygen/argon-based estimates of NCP(O<sub>2</sub>) and <sup>234</sup>Th-based estimates of particle export (2012–present). Net removal of water column nitrate (NO<sub>3</sub><sup>−</sup> removal or ΔNO<sub>3</sub>) was estimated to provide a larger-scale NCP estimate.

Aspects of the ecology and biogeochemistry of the WAP are presented in this issue and other publications (e.g. [13–15]). The marine ecosystem of the WAP extends over 1000 km along the peninsula and includes near shore coastal, continental shelf and deep slope regions, all of which experience an annual period of sea-ice cover (SIC [16]). The SIC is subject to significant regional and interannual variability, as addressed by the sampling grid used in this study. The uncertainty of specifying the initiation and duration of the illuminated production season imposed by variability in SIC at any given location is shown to be a major challenge in understanding the relationship between processes manifested over different scales of measurement. In comparing these production and removal processes, we test the null hypothesis that there was no difference among New P, NCP(O<sub>2</sub>) and Export (<sup>234</sup>Th), within years and averaged across the study region. From this it follows that, if export and new (net) production did not differ within the time frame of our observations, there would be insignificant accumulation of organic matter. We suggest that

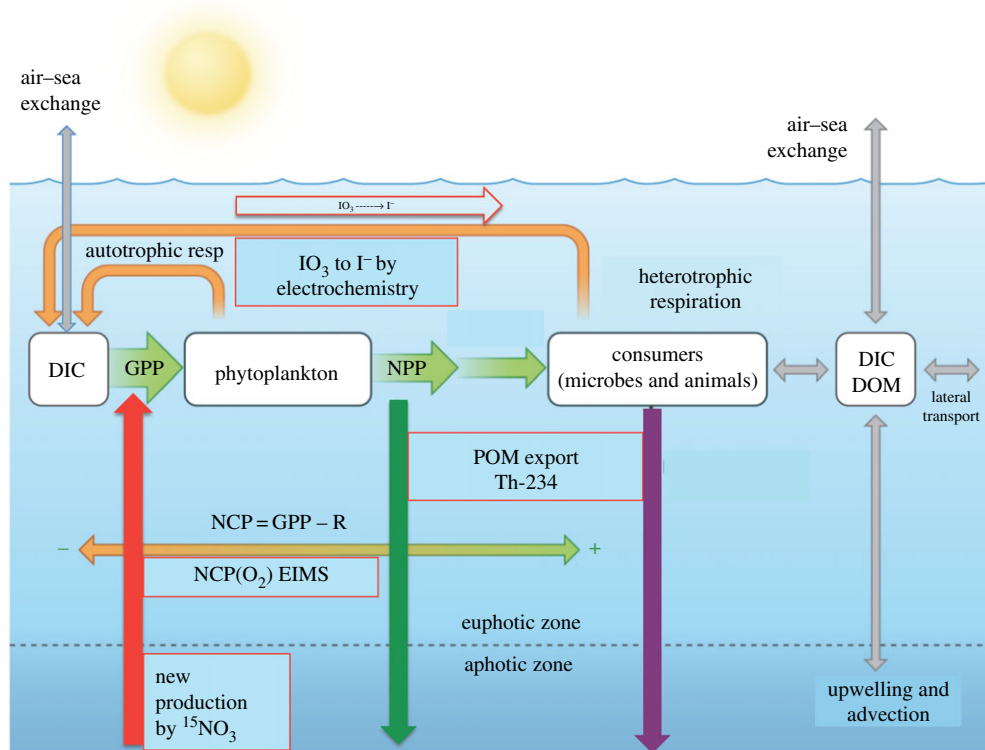


**Figure 1.** Surface ocean metabolic processes driving the balance between gross primary production and respiration. This balance is the net community production or NCP. GPP and NPP are gross and net primary production, respectively, and R is community respiration by autotrophic, heterotrophic and mixotrophic plankton. Dissolved organic matter (DOM) is produced by phytoplankton and consumers and respired by heterotrophic bacteria. Exogenous (new) nutrients (e.g. nitrogen and iron) support a varying fraction of the GPP (new production) and can be supplied or removed by both vertical and horizontal processes. The new production and NCP are available for export from the system. Atmospheric exchanges are additional source and sink terms for nutrients and organic matter supporting new production and/or export. The figure is not meant to convey the exact vertical distribution of the processes. (Modified from Ducklow & Doney [1]). (Online version in colour.)

these processes with characteristic time scales of hours to seasons, and associated space scales, are best compared over a regional scale, such as the Long Term Ecological Research (LTER) study region (electronic supplementary material, figure S1).

## 2. Methods and materials

We provide brief descriptions of the methods used for estimating each process. Details and references of individual process measurements are given in electronic supplementary material, table S1. The start of the growing season was initially taken as the last day on which SIC exceeded 15% at each sampling station [17]. Sea-ice measurements are described in Stammerjohn *et al.* [16]. Sampling for this study was conducted during annual Palmer, Antarctica LTER cruises in January (midsummer), 2012, 2013 and 2014 at 15–17 regular LTER grid stations per cruise [18], from the northern, central and southern, and coastal, shelf and slope regions along the WAP (e.g. [16,19–21]; electronic supplementary material, figure S1 and tables S2–S5). O<sub>2</sub>/Ar samples for estimating NCP(O<sub>2</sub>) were taken from the uncontaminated underway seawater supply intake at a depth of 6 m. These estimates were included at fewer stations due to the timing of instrument calibration and when the mixed layer depth (MLD) was less than 6 m. For other estimates, five discrete

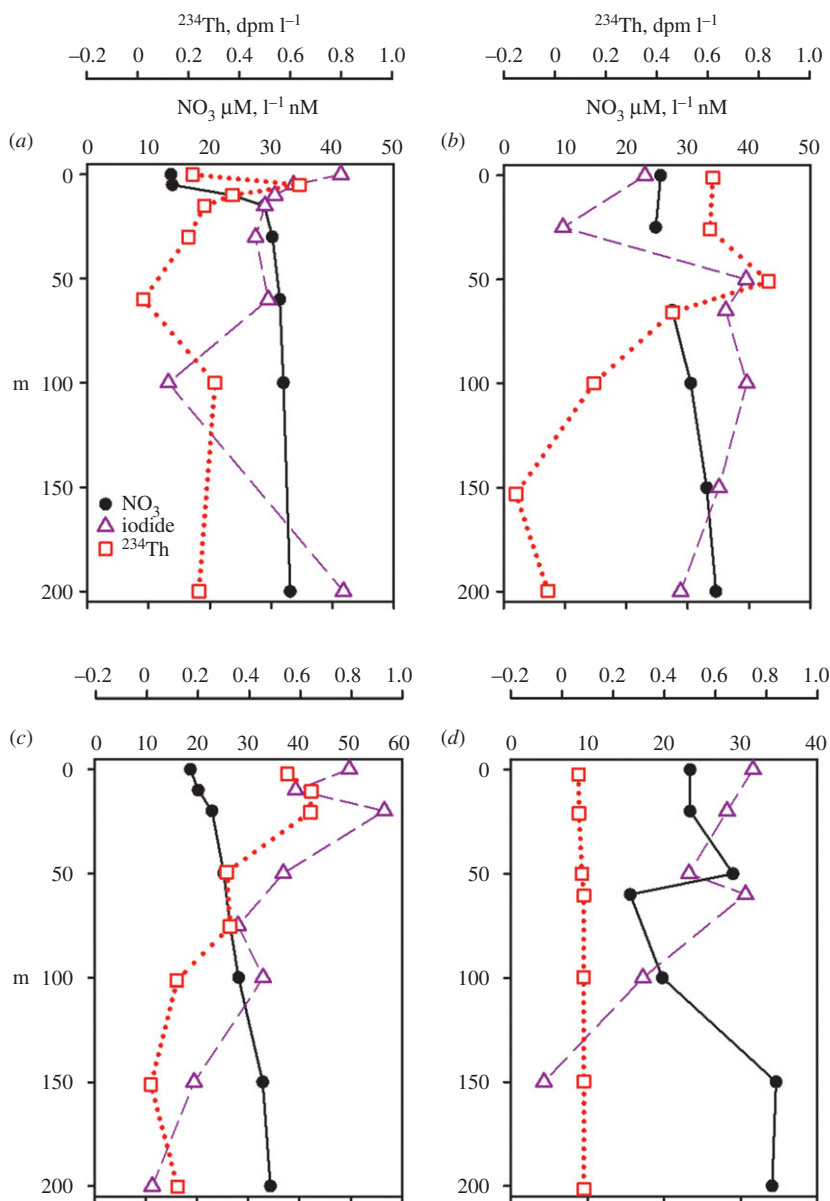


**Figure 2.** Vertical profiles of nitrate, iodide and the thorium-234 deficiency at the four corners of the sampling region in January 2012. (a,b) Northern stations 600.040 and 600.200. (c,d) Southern stations 200.040 and 200.200. The 0.040 (a,c) stations are coastal and the 0.200 stations are deep (greater than 3000 m) offshore stations. (Online version in colour.)

depth water samples were collected in the euphotic zone (defined as the depth of 1% surface irradiance, 30–75 m), and one or two deeper samples were obtained in the upper 150–200 m from CTD-Rosette hydrocasts using 101 Niskin bottles.

We calculated the net seasonal removal of nitrate + nitrite from the water column at each station ( $\Delta\text{NO}_3$ ) as an estimate of seasonal-scale NCP [22].  $\text{NO}_2^- + \text{NO}_3^-$  (hereafter  $\text{NO}_3$ ) inventories were integrated to 150 m, as concentrations approximated the observed wintertime value of  $33 \mu\text{M}$  below that depth (figure 2; electronic supplementary material, figure S2). Net seasonal iodide accumulation was similarly estimated from the 150 m inventory on the sampling day, assuming a  $7 \mu\text{Mol m}^{-3}$  starting concentration equivalent to the deep-water concentration [23] (see the electronic supplementary materials for additional details).

Particulate organic carbon and nitrogen export were estimated using the observed  $^{238}\text{U} : ^{234}\text{Th}$  disequilibrium over 0–150 m at each station.  $^{234}\text{Th}$  concentrations were measured using standard small volume methods [24–26].  $^{234}\text{Th}$  flux was computed using a one-dimensional steady-state equation and converted to C and N flux using a power-law relationship between C :  $^{234}\text{Th}$  and depth determined from previous measurements [26,27] (see electronic supplementary material).  $\text{NCP}(\text{O}_2)$  was derived from oxygen budgets calculated for the mixed layer at each station using dissolved oxygen normalized to argon as determined by equilibrator inlet mass spectrometry (EIMS) following Eveleth *et al.* [28] and Cassar *et al.* [29]. We used the continuous underway  $\text{NCP}(\text{O}_2)/\text{Ar}$  data of Eveleth *et al.* [28], averaged over a 15 min period around each CTD-Rosette station at which bottle sampling was also conducted. Eveleth *et al.* [28] did not include in their dataset negative  $\text{NCP}(\text{O}_2)$  results, because of the possibility of advection or mixing of low oxygen water into the mixed layer contaminating the biological signal. These results, including  $\text{NCP}(\text{O}_2) < 0$ , are reported in electronic supplementary material, tables S3–S5. The presence or absence of negative  $\text{NCP}(\text{O}_2)$  values did not alter the statistical relationships between  $\text{NCP}(\text{O}_2)$  and the other processes. Inclusion or exclusion of one extremely high  $\text{NCP}(\text{O}_2)$  value (36.5  $\text{mmol N m}^{-2} \text{d}^{-1}$  at Station 600.040 in 2014; electronic supplementary material, table S5 and figure 7) did not change the statistical results. New production rates (New P) were estimated in 24 h deck incubations with  $^{15}\text{NO}_3$  [27]. Net primary production rates (NPP  $^{14}\text{C}$ ) were estimated by 24 h deck incubations with  $^{14}\text{C}$ -bicarbonate [30]. For comparison, all values were converted to nitrogen-based units using the Redfield ratio 106 C : 16 N :  $-138 \text{O}_2$  [27].

### 3. Results and discussion

#### (a) Sea-ice cover and net changes in the nitrate and iodide inventories

As the sun ascends in spring, and as sea ice begins to melt and retreat, solar irradiance and stratification increase in the upper water column, triggering phytoplankton blooms and initiating net removal of dissolved inorganic carbon (DIC) [22], nitrate, silicate and phosphate [31], and net production of oxygen and iodide (see below, [23]). At some point following the ice retreat, particulate matter export builds to its annual peak [32]. Unlike Sweeney *et al.* [22], we do not have early-season observations and had to estimate a date when net production started. Sweeney *et al.*'s observations were made just prior to the opening of the Ross Sea Polynya in October–November 1996, providing start dates and direct observations of early-season nitrate and DIC inventories to use as start values for seasonal-scale inventory changes. In our study, retreating sea ice passed 50% and 15% SIC on average on days  $330 \pm 28$  and  $346 \pm 27$ , respectively, in 2012–2014, electronic supplementary material, table S2. The 15% and 50% SIC days at our stations, electronic supplementary material, tables S3–S5, are significantly correlated ( $\text{day } 50\% = 0.84 \times \text{day } 15\% + 39.03$ ,  $r = 0.83$ ;  $p < 0.001$ ,  $n = 49$  stations). The number of days from ice retreat (15% SIC) until sampling averaged 51, 37 and 6 in 2012, 2013 and 2014, respectively (electronic supplementary material, table S3–S5); 2014 was the largest positive ice anomaly since 1987–1988. Late ice retreat in 2014 (electronic supplementary material, figure S3), left many stations still ice-covered at the time of sampling and prevented access to some stations. At six of 17 stations, the subsequent ice retreat yielded negative days since retreat (e.g. electronic supplementary material, table S5).

Vertical profiles of  $\text{NO}_3$  show 10–15  $\mu\text{M}$  reductions in surface concentration (figure 2; electronic supplementary material, figure S2), and some stations were nearly depleted at the surface in 2013. The average inventories (0–150 m) were 4203, 4386 and 4229  $\text{mmol N m}^{-2}$  in 2012–2014, representing a 12–15% depletion below the average winter inventory of 4977  $\text{mmol N m}^{-2}$ . Using the 15% SIC criterion for the date of ice retreat and the assumed start of net utilization gave an average nitrate removal rate of 13.5 (range 9–18) and 20 (range 9–32)  $\text{mmol N m}^{-2} \text{d}^{-1}$  in 2012 and 2013. In 2014, the heavy ice cover retreated from many stations only shortly before or even after our occupations, yielding either very high positive rates, when ice retreat was only a few days prior to sampling, or negative rates if it followed. However, the observed inventories in 2014 were

actually the same as in the preceding years. This observation suggests that our assumed starting value for  $\text{NO}_3$  removal was in error and that net removal started some time before the 15% SIC criterion, i.e. under heavy ice cover. To take into account of this possibility, we used October 1 as a date for the presumed start of the net growing season, based on time series observations of SIC, chlorophyll and nutrients near Palmer Station [31]. Rates of nitrate removal derived using days since October 1 were similar in the 3 years, and lower than the 15% and 50% SIC rates (electronic supplementary material, tables S3–S5).

## (b) Iodate reduction

Iodate reduction to iodide in the euphotic zone is a biogeochemical process that is related to primary production, although not necessarily directly driven by it. Once formed, iodide is only very slowly oxidized on timescales of months or longer [33]. The build-up of iodide in the surface mixed layer has, therefore, been proposed as a means of estimating seasonally integrated productivity, or related parameters such as nitrate uptake, in the sense of integrating because the water column was last zeroed by vertical mixing, typically in winter [23,33–36]. The conversion of iodate to iodide is associated with phytoplankton growth and primary production and is the major iodine transformation pathway in the ocean. In comparison, uptake of iodine into phytoplankton cells and subsequent export by sinking is a secondary pathway accounting for only a small fraction of the ocean iodine cycle. It has been suggested that the reduction of iodate to iodide takes place outside the cell, likely on the cell surface. It is not clear if the build-up of iodide will reflect new, net or gross productivity [33]. We, therefore, obtained a new set of samples in 2012 to evaluate and calibrate the iodide productivity proxy against the other processes.

Vertical profiles of iodide demonstrated a general pattern of accumulation above the deep-water background (figure 2; electronic supplementary material, figure S2). Discrete depth iodide concentrations are significantly correlated with nitrate and also weakly but significantly correlated with the  $^{234}\text{Th}$  deficit (figure 3). The iodide versus nitrate plot indicates a good correlation with a slope and intercept similar to that derived from a global scale dataset for waters with surface nitrate concentrations above  $2\ \mu\text{M}$  [33], suggesting the global relationship applies in the WAP. The better correlation of iodide accumulation with nitrate rather than  $^{234}\text{Th}$  deficiency suggests that the mechanisms controlling iodine removal and the associated carbon biogeochemistry processes are related to those that directly cycle carbon and nitrogen via primary production rather than export.

The average integrated iodide build-up through the top 150 m of the water column is  $4.6 \pm 0.8\ \text{mmol m}^{-2}$ . The average iodide concentration at 200 m is low,  $7.4 \pm 3.5\ \text{nM}$ , but well above the detection limit and we assume this represents the winter surface water iodide background concentration (see the electronic supplementary material). We, therefore, correct the upper 150 m integrated iodide inventory for this background to give a value of the seasonal iodide build-up between winter mixing and the time of sampling of  $3.5\ \text{mmol m}^{-2}$ . Chance *et al.* [23] measured the build-up of iodide at the Rothera site in Marguerite Bay in the southern part of the station grid (near Station line 200, cf. electronic supplementary material, figure S1) and over 1 year found a good relationship (although substantially lagged in time) with integrated  $^{14}\text{C}$ -based PP and an  $I/C$  assimilation ratio of  $0.16 \times 10^{-3}\ \text{mol mol}^{-1}$ . The use of the  $0.16 \times 10^{-3}\ I/C$  ratio results in an estimate of seasonal production of  $3.3\ \text{mol N m}^{-2}$  that is much higher than the other estimates made here and so instead we use the conversions based on the observed iodide nitrate relationship ( $-266\ \text{mol N} : \text{mol I}$ ; figure 3).

## (c) Comparison of production and removal processes

Here we compare the magnitudes and variability among the different production ( $\text{NCP}(\text{O}_2)$ ,  $\text{NPP}$  ( $^{14}\text{C}$ ),  $\text{New P}$ ) and particle export rates ( $^{234}\text{Th}$ ) measured in the region during 2012–2014. We address two main issues: first, the comparison between shorter-term processes (hours–days) and longer-term (weeks–months) nitrate removal estimates (electronic supplementary material,

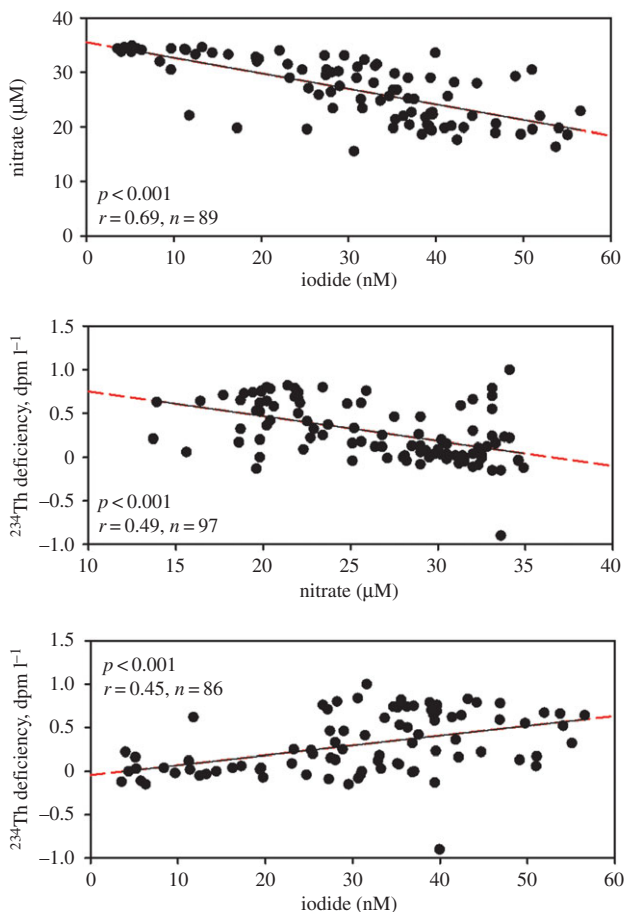


**Figure 3.** Scatterplots of discrete depth  $[\text{NO}_2 + \text{NO}_3]$ , iodide concentrations and thorium-234 deficiencies relative to uranium-238 in January 2012. The iodide–nitrate relationship is discussed in the text. (Online version in colour.)

table S1); and second, the grid-scale balance between New P or  $\text{NCP}(\text{O}_2)$  and Export ( $^{234}\text{Th}$ ) in the midsummer period. Comparison of the *measurements* (as contrasted with the *processes*) is addressed in the electronic supplementary material.

NPP rates as estimated by 24-h deck incubations with  $^{14}\text{C}$  were moderate in 2012 ( $7.8 \text{ mmol N m}^{-2} \text{ d}^{-1}$ ) and over twice as high in 2013 and 2014 (electronic supplementary material, tables S3–S5). Corresponding rates of Export ( $^{234}\text{Th}$ ), NPP ( $^{14}\text{C}$ ), New P and  $\text{NCP}(\text{O}_2)$  are reported in electronic supplementary material, tables S3–S5 and their spatial and interannual (2012–2014) variability within the original sampling grid are depicted in figures 4–7. Within-year variability was moderately high for all the rate processes: the average of the mean coefficients of variation (s.d./mean) for each of the four rate processes was 1.2 over the 3 years of this study. This within-year variability is some combination of spatial (10–100 km) and temporal (1–20 d) variability within the sampling grid in the midsummer period. Sampling was conducted over 12–15 days each January (electronic supplementary material, tables S3–S5). This is about the time scale of a phytoplankton bloom and of the Export ( $^{234}\text{Th}$ ) (approximately 20 d) and  $\text{NCP}(\text{O}_2)$  (approx. 10 d) estimates, and similar to the time scale of sea-ice retreat from 50% to 15% ice cover (electronic supplementary material, table S2). NPP ( $^{14}\text{C}$ ) and New P measurements are made over 24 h and are subject to shorter-term forcing. Rates will likely be higher on sunny than cloudy days, making it hard to disentangle temporal and spatial variability. We believe that we achieve reasonable ‘snapshots’ of grid-averaged rate processes characteristic of early to midsummer in the WAP region. As a result of within-year spatio-temporal variability, New P,  $\text{NCP}(\text{O}_2)$  and Export

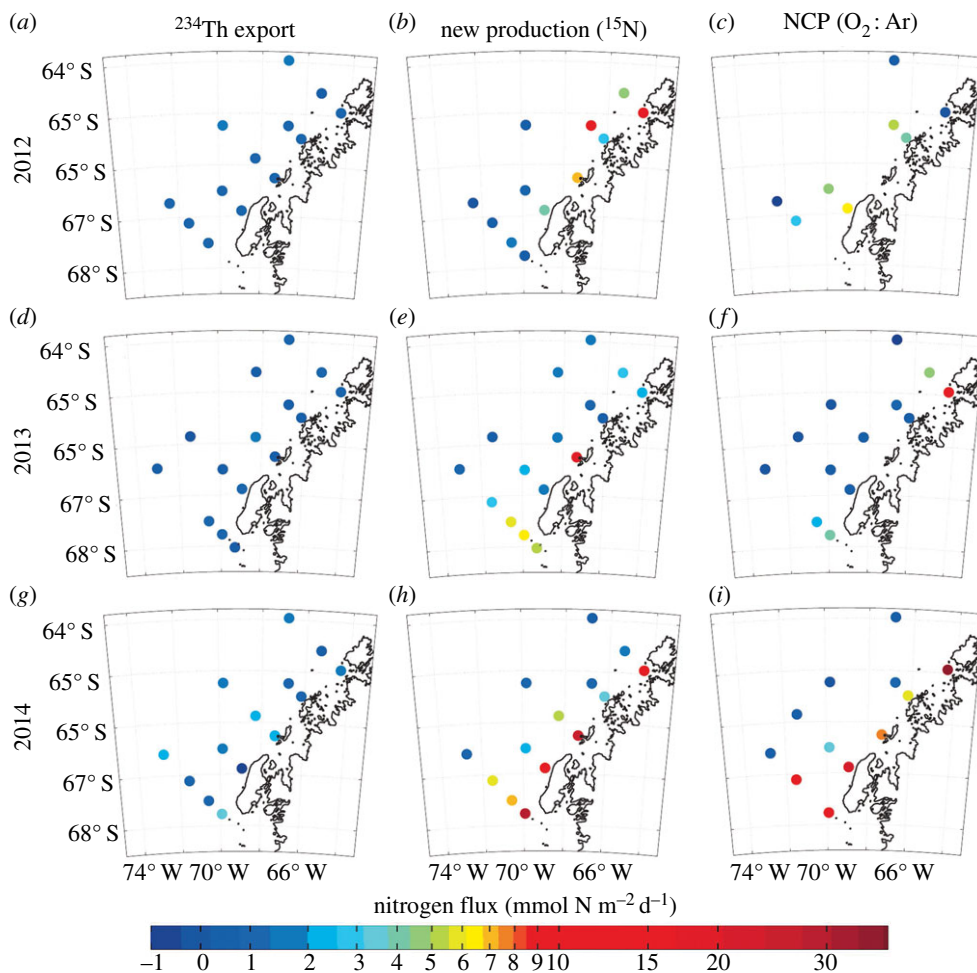


**Figure 4.** (a–i) Distribution of rates of export, new production (nitrate uptake) and NCP( $O_2$ ) along the WAP in January, 2012–2014. (Online version in colour.)

( $^{234}\text{Th}$ ) did not differ significantly across years (i.e. estimates of each individual process did not differ across the 3 years 2012–2014;  $t$ -tests, all greater than 0.05, data collated from electronic supplementary material, tables S3–S5).

These variables did, however, differ from one another within years. Export ( $^{234}\text{Th}$ ) was consistently low across the study area in 2012–2014 relative to our other measurements (figure 4). The positive export values ranged from 0.2 to  $3.9 \text{ mmol N m}^{-2} \text{ d}^{-1}$  with most values clustering around  $1 \text{ mmol N m}^{-2} \text{ d}^{-1}$  (electronic supplementary material, tables S3–S5). Similar to other observations [37], the deep, ‘oceanic’ off-shelf stations did not have lower export rates than the coastal and shelf stations when integrated to 150 m. The 150 m integration depth masks a pattern of higher mixed layer export ( $^{234}\text{Th}$ ) near the coast with higher subsurface  $^{234}\text{Th}$  remineralization above 150 m (figure 2). By contrast, on-to-offshore and north to south gradients are apparent for new and net community production rates (figure 4; see also fig. 3 in [28]). North to south gradients are associated with ice edge blooms encountered in the south part of the study area later in the summer cruises (cruises proceed from north to south). Ice retreat also has a north-to-south progression [16], and thus it is more likely that ice edge blooms triggered by ice retreat will be encountered to the south [38]. Continuous NCP( $O_2$ ) estimates reveal high NCP rates in the south in 2013–2014 and in the coastal region in all 3 years [28].

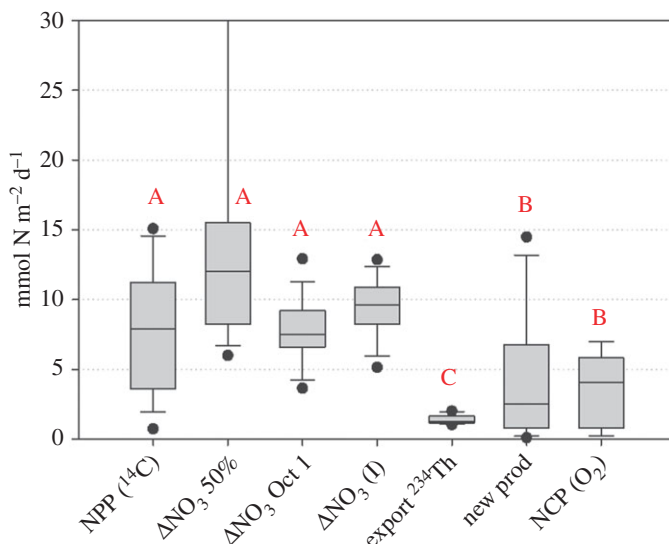


**Figure 5.** Box plots of production and export rates along the WAP shelf in January 2012. Each box represents the water column integrated data from all the stations as given in electronic supplementary material, table S3. (NPP ( $^{14}\text{C}$ ): rates of daily net primary production;  $\Delta\text{NO}_3$ : average daily rates of  $\text{NO}_3$  removal for the specified ice retreat criteria;  $\Delta\text{NO}_3\text{-I}$ :  $\text{NO}_3$  removal converted from iodide inventory accumulation; export ( $^{234}\text{Th}$ ): daily export rate from  $^{234}\text{Th}$ ; New Prod: daily rate from  $^{15}\text{NO}_3$  incorporation; NCP( $\text{O}_2$ ): daily rate of NCP from mixed layer  $\text{O}_2$  budget as measured by EIMS. The top and bottom of the boxes show the 75% and 25% percentiles, respectively. The capped vertical lines indicate the 90th and 10th percentiles and symbols indicate outliers. The line inside the box is the median. Rates sharing letters are not statistically different averaged over the sampling region within each year ( $T$ -test,  $p > 0.05$ ). Rates with different letters are significantly different ( $p < 0.05$ ). All values were converted to nitrogen equivalents as described in Methods and materials. (Online version in colour.)

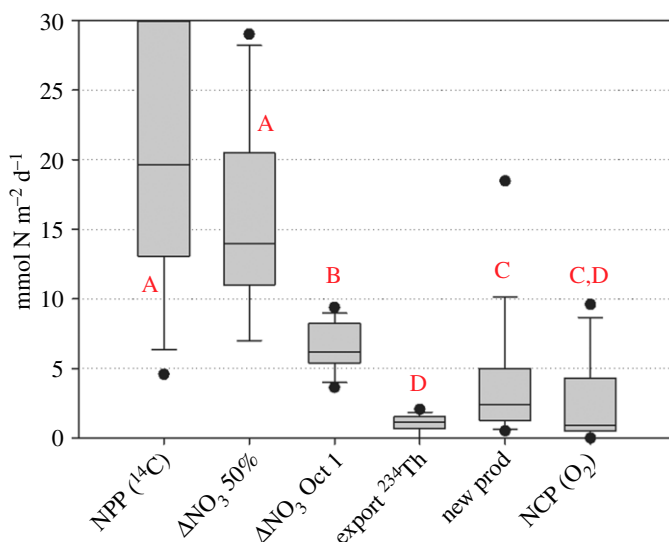


**Figure 6.** Box plots of production and export rates along the WAP shelf in January 2013 as in figure 5 with data from electronic supplementary material, table S4. Iodide was not measured in 2013. (Online version in colour.)

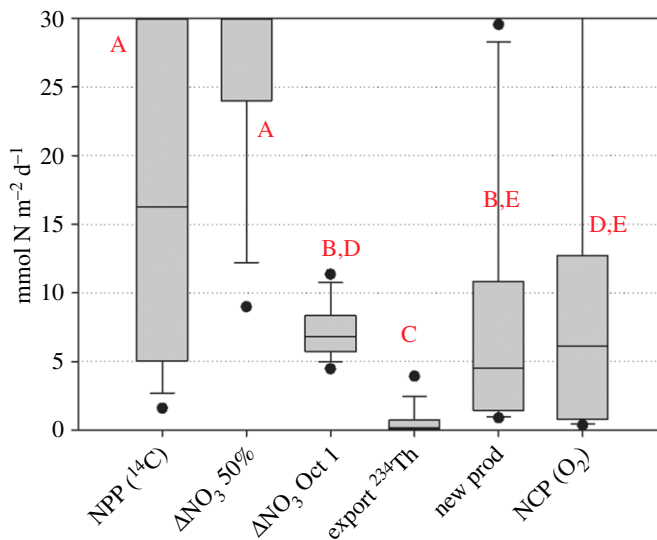


**Figure 7.** Box plots of production and export rates along the WAP shelf in January 2014 as in figure 6, with data from electronic supplementary material, table S5. Iodide was not measured in 2014. (Online version in colour.)

We expected that the longer-timescale estimates of seasonal net nitrate removal (normalized to per d units) would be lower than the other estimates, especially the short-term, biological uptake rate measurements ( $^{14}\text{C}$ ,  $^{15}\text{NO}_3$ ) made in midsummer. This is because the seasonal-scale estimates include the beginning of the season when rates are lower due to low solar irradiance. This is not what we observed [28]. Rate comparisons are shown in figures 5–7. In each year, the seasonal net nitrate depletion rate derived from the 50% SIC retreat criterion (which is lower than the rate derived from the 15% SIC criterion) were not significantly different from the short-term  $^{14}\text{C}$ -based rates of primary production, and greater than the rates of new production, Export ( $^{234}\text{Th}$ ) and NCP( $\text{O}_2$ ) in all 3 years. Using 1 October as the start of the production season gave lower daily rates than the 50% SIC-based estimate; however, these too were greater than the rates of new production, NCP( $\text{O}_2$ ) and Export ( $^{234}\text{Th}$ ) in 2012 and 2013. Considering the ice retreat timing, in 2012 and 2013, the peak of the bloom likely occurred greater than 10 days prior to the cruise. Short-term  $\text{O}_2/\text{Ar}$ -based estimates would not capture that productivity, while nitrate removal would. The results in figure 7 (2014) suggest that there must have been bloom activity significantly prior to the 50% ice retreat and that the NCP( $\text{O}_2$ ) rate remained consistently high over the growing season.

Net nitrate removal is often used as a larger-scale or longer-term estimate of new production and NCP [39,40]. Seasonal estimates of DIC removal were about three times greater than January  $\text{O}_2/\text{Ar}$ -based NCP estimates [28], consistent with our results for the  $\text{NO}_3$  inventory. One interpretation of the high daily nitrate removal rates is that the greater part of the bloom activity was completed before the cruise, and the net removal rates reflect sustained high rates of removal during blooms in the weeks to months preceding the cruises. Indeed, in a five-month study including  $\text{NO}_3$  removal and uptake near Palmer Station (northeastern portion of our study region) in 2012–2013, Stukel *et al.* [27] found excellent agreement between  $\text{NO}_3$  removal and uptake, although both peaked in late November; hence measurements of net seasonal  $\text{NO}_3^-$  removal made only in January (but integrating over the productive early season) would overestimate contemporaneous  $\text{NO}_3$  uptake measurements. Similarly, Bowman *et al.* [41] found that phytoplankton blooms occurred at Palmer and Rothera Stations in December, 2011 and 2012, prior to the January 2012 and 2013 cruises (see also fig. 2 in [28]). The bloom phenologies at these shallow near shore sites may not reflect the timing of blooms on the offshore grid. A corollary of this interpretation is that the shorter-term estimates made during the cruises mainly represent

post-bloom conditions with lower average rates and possibly greater reliance of the production system on regenerated nutrients, and with lower  $f$ -ratios. The near shore bloom was 15–30 days later (December–January) in 2013–2014, coinciding with the cruise, and when ice cover retreated later than in the preceding 2 years (electronic supplementary material, figure S3, [28]).

#### (d) Balance between production and export

Next, we compare the January estimates of NCP(O<sub>2</sub>), New P and Export (<sup>234</sup>Th), the balance between production and removal, and temporal offsets between these processes. It is important to understand that, when making these comparisons, the <sup>234</sup>Th-based estimates of particle export only address sinking particles, and do not include other export processes such as mixing of DOM or suspended particulate matter [42]. Estimates of sinking particle export derived from the <sup>238</sup>U : <sup>234</sup>Th disequilibrium were lower than new production rates in all 3 years (2012–2014) and were less than NCP(O<sub>2</sub>) in 2012 and 2014. The relative magnitudes of these rates varied greatly at individual stations (electronic supplementary material, tables S3–S5). Any of the three processes could exceed the other two at any given station. On average, however, <sup>234</sup>Th-based export was about one-fifth to one-half of the other two rate estimates. The consistency of these grid-average estimates, in the face of high spatial (station to station) variability, and across years differing very greatly in SIC, suggests a significant perennial imbalance between production and sinking particle export during the midsummer period. We consider potential reasons for this imbalance below.

Observations of production–export imbalances are not uncommon in aquatic and terrestrial ecosystems [2,12,43]. Most such cruise-based estimates are made over relatively brief time periods of a few weeks at most. A steady-state balance should exist over some suitably large time and space scales, but there is no *a priori* reason that these rates have to balance over periods shorter than about a year, or over areas smaller than an ocean basin. Before pursuing temporal imbalance further, we briefly address the possibility of systematic over- or underestimation of new production and export. Estapa *et al.* [12] tested the hypothesis that spatial offsets at submesoscales could lead to imbalances between production (NCP) and particle export. They observed that densely sampled NCP and export (approx. 2 km station spacing) were correlated over larger spatial scales (30–40 km), but paired observations at individual stations were not. Our data are reported at widely spaced intervals (100 by 50 km in a 400 × 200 km domain; figure 5), so we believe that spatial offsetting is likely to be averaged out in our sampling design. Eveleth *et al.* [27] showed that the decorrelation length scales for biological properties over the shelf is quite short, on the order of 5 km.

The  $f$ -ratios (ratio of New P/NPP) and  $e$ -ratios (Export/NPP) constitute a check on the relative magnitudes of the New P and Export (<sup>234</sup>Th) rates (electronic supplementary material, table S6). The geometric mean  $f$ - and  $e$ -ratios for 2012 were  $0.37 \pm 0.32$  and  $0.18 \pm 0.67$ , not unusual values for polar seas [27,44,45]. The  $e$ -ratios were lower in 2013 and 2014 ( $0.05 \pm 0.05$  and  $0.11 \pm 0.18$ ). The measured Export (<sup>234</sup>Th) rates were  $1.4 \pm 0.3$ ,  $1.1 \pm 0.6$  and  $1.8 \pm 1.2$  mmol N m<sup>-2</sup> d<sup>-1</sup> in 2012–14, respectively; and not significantly different between years ( $t$ -tests,  $p > 0.05$ ). On the other hand, the NPP (<sup>14</sup>C) rates were very high in 2013 and 2014 ( $27 \pm 23$  and  $25 \pm 26$ , respectively). The  $e$ -ratios were low in 2013 and 2014 because the primary production rates were very high, not because the export rates were unusually low. Whether or not the export rates were lower than expected given the high NPP (<sup>14</sup>C) rates is an interesting question that cannot be answered with this dataset. The  $f$ -ratios exhibited the same temporal pattern as the  $e$ -ratios: relatively high in 2012 (mean ratio  $0.37 \pm 0.32$  in 2012 and lower in 2013 and 2014 ( $0.11 \pm 0.11$  and  $0.24 \pm 0.13$ ), respectively; electronic supplementary material, table S6).

There are few measurements of  $e$ - and  $f$ -ratios in the WAP or other Antarctic marginal ice zones for comparison with these observations. Huang *et al.* [46] estimated  $f$ -ratios ranging from 0 to 0.83, based on discrete O<sub>2</sub>/Ar and triple oxygen isotope measurements.  $e$ -ratios derived from moored sediment traps are not directly comparable because even the shallowest collections are often from greater depths and do not directly address export from the productive surface layer. Such estimates are usually low [32], and it has been shown that moored traps tend to suffer from

an undercollection bias [47]. Another possible reason for low  $f$ -ratios could be that  $\text{NO}_3$  uptake was iron-limited rather than nitrate-limited in midsummer in the WAP [48]. Available dissolved iron concentrations are variable on the WAP shelf [49].

Finally, we estimate turnover rates for the standing stock of accumulated particulate organic nitrogen (PN) in 2012, from PN measurements and the New P rates (PN data are not available for 2013–2014). Both particulate and semilabile dissolved organic carbon (DOC) accumulated in the upper 150 m (electronic supplementary material, table S7). PN accumulations averaged  $115 \pm 46 \text{ mmol N m}^{-2} \text{ d}^{-1}$  (range 41–184  $\text{mmol N m}^{-2} \text{ d}^{-1}$ ). We estimated semilabile dissolved organic nitrogen (DON) from DOC using a DOC:DON molar ratio of 11.5 [50]. Semilabile DON accumulation averaged  $39 \pm 12 \text{ mmol N m}^{-2} \text{ d}^{-1}$  (range 18–60), or 37% the stock of PN. The size of the accumulated PN pool can be scaled by normalizing to the rate measurements. For example it represents about 17 days of primary production at the average level observed in 2012 (with one high value of 200 removed; electronic supplementary material, table S7). Similarly, this accumulated stock would take on average 84 days to be removed at the observed rates of Export ( $^{234}\text{Th}$ ) (range 33–159 days). Similar comparisons can be made using new production and  $\text{NCP}(\text{O}_2)$ . This suggests a substantial imbalance in the production/export system along the WAP.

Our measurements are snapshots, and do not address the issue of temporal imbalance or horizontal advection. The Palmer LTER sediment trap moored at 170 m depth near station 600.100 reveals strong seasonality in particle flux, in common with earlier observations at this site [51]. The peak flux captured by the LTER trap occurs anytime between mid-December and mid-February [32], so our observations in 2012–2014 could be anywhere along the bloom-sequence. In 2012, there was a broad flux peak between 6 January and 16 March. In the 2012–2013 season corresponding to the January 2013 observations, a very brief flux peak occurred in December 2012 (unpublished data in Palmer Datazoo, dataset 26; 2014 data not yet available).

Temporal imbalance was likely partially responsible for the large New P-Export ( $^{234}\text{Th}$ ) imbalance measured during the 2014 cruise, which was sampled during a delayed spring bloom. In contrast to the annual offshore cruises each January that comprise these datasets, daily to weekly estimates of nitrate removal, New P and  $\text{NCP}(\text{O}_2)$  and Export ( $^{234}\text{Th}$ ) were made throughout the growing season in the near shore region at Palmer Station. Stukel *et al.* [27] observed a good temporal correspondence between  $^{15}\text{NO}_3$  uptake (New P) and net removal of the  $\text{NO}_3$  stock during the 2012–2013 season, but Export ( $^{234}\text{Th}$ ) was much lower. Similarly, Tortell *et al.* [52] obtained continuous estimates of  $\text{NCP}(\text{O}_2)$  over the same period. Both sets of observations captured the spring bloom in November–December. Even when integrated over the full October to March productive season, there was a large excess of production over export by sinking particles. Stukel & Ducklow [42] suggested that nearly half of the organic nitrogen exported from the WAP surface ocean by the biological pump may be transported by vertical mixing of suspended particles that would not be measured by  $^{234}\text{Th}$  disequilibrium approaches. Furthermore, their results showed that vertical mixing was more important in the productive shelf regions, where we find greater imbalance between new and export production.

## 4. Conclusion

Taken together, our results add to a growing body of literature showing that new and net community production are high in the WAP, but that they are not balanced by the sinking flux of particles measured by sediment traps or  $^{238}\text{U} : ^{234}\text{Th}$  disequilibrium [27,44,47]. Our specific result of good agreement between  $^{15}\text{NO}_3$  uptake new production measurements and  $\text{O}_2 : \text{Ar}$ -based  $\text{NCP}$  measurements (cruise averages always agreed to within a factor of 2), give us good confidence that the new production–export imbalance results not from a methodological bias, but in fact reflects the reality of an ecosystem in which other processes (vertical mixing, active transport by vertically migrating zooplankton, removal by migratory whales and seabirds) are important components of the biological pump. Quantifying these alternate mechanisms of export, along with their spatio-temporal variability and differential responses to secular warming in the WAP, should be considered a priority for further research.

**Data accessibility.** Data are made available in the Palmer LTER DataZoo (<http://pal.lternet.edu/data>).

**Authors' contributions.** H.W.D. conceived this study with input from S.C.D., supervised the fieldwork and drafted the manuscript. T.J., A.R.B., J.B. and R.C. collected and interpreted the iodide data. M.R.S. obtained the thorium-234 data and R.E. and N.C. provided the NCP(O<sub>2</sub>) data. R.E. and M.R.S. helped draft the manuscript. O.S. contributed the NPP (<sup>14</sup>C) data. T.J. helped edit the manuscript. H.W.D., R.E., M.R.S. and T.J. critically read the manuscript and gave final approval for publication.

**Competing interests.** We have no competing interests.

**Funding.** This research was supported by US National Science Foundation grants OPP-0823101 and PLR-1440435 (Palmer Long Term Ecological Research) and OPP-1340886. T.J., R.C., A.R.B. and J.B. were supported by grants from the UK NERC NE/F017359/1, NE/G016585/1 and NE/H00548X/1. N.C. was supported by NSF OPP-1043339 and NSF OPP-1643534. R.E. was supported by National Science Foundation, Graduate Research Fellowship Program under grant 1106401. A portion of this work was performed at the National High Magnetic Field Laboratory, which is supported by National Science Foundation Cooperative Agreement no. DMR-1644779 and the State of Florida. H.W.D. was supported in part by a gift from the Vetlesen Foundation.

**Acknowledgement.** We thank the officers and crew of ARSV Laurence M Gould for many years of support of our research.

## References

1. Ducklow HW, Doney SC. 2013 What is the metabolic state of the oligotrophic ocean? A debate. *Ann. Rev. Mar. Sci.* **5**, 525–533. (doi:10.1146/annurev-marine-121211-172331)
2. Chapin III FS *et al.* 2006 Reconciling carbon-cycle concepts, terminology, and methods. *Ecosystems* **9**, 1041–1050. (doi:10.1007/s10021-005-0105-7)
3. Williams PJ. 1998 The balance of plankton respiration and photosynthesis in the open oceans. *Nature* **394**, 55–57. (doi:10.1038/27878)
4. Williams PJ, Bowers DG. 1999 Regional carbon imbalances in the oceans. *Science* **284**, 1735. (doi:10.1126/science.284.5421.1735b)
5. Williams PJB, Quay PD, Westberry TK, Behrenfeld MJ. 2013 The oligotrophic ocean is autotrophic. *Ann. Rev. Mar. Sci.* **5**, 551–569. (doi:10.1146/annurev-marine-121211-172337)
6. Eppley RW, Peterson BJ. 1979 Particulate organic matter flux and planktonic new production in the deep ocean. *Nature* **282**, 677–680. (doi:10.1038/282677a0)
7. Longhurst A. 1995 Seasonal cycles of pelagic production and consumption. *Prog. Oceanogr.* **36**, 77–167. (doi:10.1016/0079-6611(95)00015-1)
8. Dugdale RC, Goering JJ. 1967 Uptake of new and regenerated forms of nitrogen in primary production. *Limnol. Oceanogr.* **12**, 196–206. (doi:10.4319/lo.1967.12.2.0196)
9. Legendre L, Gosselin M. 1989 New production and export or organic matter to the deep ocean: consequences of some recent discoveries. *Limnol. Oceanogr.* **34**, 1374–1380. (doi:10.4319/lo.1989.34.7.1374)
10. Laws EA. 1991 Photosynthetic quotients, new production and net community production in the open ocean. *Deep Sea Res.* **38**, 143–167. (doi:10.1016/0198-0149(91)90059-O)
11. Hamme RC *et al.* 2012 Dissolved O<sub>2</sub>/Ar and other methods reveal rapid changes in productivity during a Lagrangian experiment in the Southern Ocean. *J. Geophys. Res. Oceans* **117**, C00F12. (doi:10.1029/2011JC007046)
12. Estapa ML, Siegel DA, Buesseler KO, Stanley RHR, Lomas MW. 2015 Decoupling of net community and export production on submesoscales in the Sargasso Sea NCP and export at submesoscales. *Glob. Biogeochem. Cycles* **29**, 1266–1282. (doi:10.1002/2014GB004913)
13. Ducklow HW, Baker K, Martinson DG, Quetin LB, Ross RM, Smith RC, Stammerjohn SE, Vernet M, Fraser W. 2007 Marine ecosystems: the West Antarctic Peninsula. *Phil. Trans. R. Soc. Lond. B* **362**, 67–94. (doi:10.1098/rstb.2006.1955)
14. Ducklow HW *et al.* 2012 The Marine Ecosystem of the West Antarctic Peninsula. In *Antarctica: An extreme environment in a changing world* (eds A Rogers, N Johnston, A Clarke, E Murphy), pp. 121–159. London, UK: Blackwell.
15. Ross RM, Quetin LB, Lascara CM. 1996 Distribution of Antarctic krill and dominant zooplankton west of the Antarctic Peninsula. In *Foundations for ecological research west of the antarctic peninsula* (eds RM Ross, EE Hofmann, LB Quetin), pp. 199–217. Washington, DC: American Geophysical Union.

16. Stammerjohn SE, Martinson DG, Smith RC, Iannuzzi SA. 2008 Sea ice in the western Antarctic Peninsula region: spatio-temporal variability from ecological and climate change perspectives. *Deep Sea Res. II* **55**, 2041–2058. (doi:10.1016/j.dsr2.2008.04.026)
17. Ducklow HW, Wilson SE, Post AF, Stammerjohn SE, Erickson M, Lee S, Lowry KE, Sherrell RM, Yager PL. 2015 Particle flux on the continental shelf in the Amundsen Sea Polynya and Western Antarctic Peninsula. *Elementa* **3**, 000046.
18. Waters KJ, Smith RC. 1992 Palmer LTER: a sampling grid for the palmer LTER program. *Antarct. J. USA* **27**, 236–239.
19. Martinson DG, Stammerjohn SE, Iannuzzi RA, Smith RC, Vernet M. 2008 Western Antarctic Peninsula physical oceanography and spatio-temporal variability. *Deep Sea Res. II* **55**, 1964–1987. (doi:10.1016/j.dsr2.2008.04.038)
20. Ducklow HW, Schofield O, Vernet M, Stammerjohn S, Erickson M. 2012 Multiscale control of bacterial production by phytoplankton dynamics and sea ice along the western Antarctic Peninsula: A regional and decadal investigation. *J. Mar. Sys.* **98–99**, 26–39. (doi:10.1016/j.jmarsys.2012.03.003)
21. Steinberg DK *et al.* 2015 Long-term (1993–2013) changes in macrozooplankton off the Western Antarctic Peninsula. *Deep Sea Res. I* **101**, 54–70. (doi:10.1016/j.dsr.2015.02.009)
22. Sweeney C, Hansell DA, Carlson CA, Codispoti LA, Gordon LI, Marra J, Millero FJ, Smith WO, Takahashi T. 2000 Biogeochemical regimes, net community production and carbon export in the Ross Sea, Antarctica. *Deep-Sea Research II* **47**, 3369–3394. (doi:10.1016/S0967-0645(00)00072-2)
23. Chance R *et al.* 2010 Seasonal and interannual variation of dissolved iodine speciation at a coastal Antarctic site. *Mar. Chem.* **118**, 171–181. (doi:10.1016/j.marchem.2009.11.009)
24. Benitez-Nelson CR, Buesseler KO, van der Loeff MR, Andrews J, Ball L, Crossin G, Charette MA. 2001 Testing a new small-volume technique for determining Th-234 in seawater. *J. Radioanal. Nucl. Chem.* **248**, 795–799. (doi:10.1023/A:1010621618652)
25. Pike SM, Buesseler KO, Andrews J, Savoye N. 2005 Quantification of <sup>234</sup>Th recovery in small volume sea water samples by inductively coupled plasma-mass spectrometry. *J. Radioanal. Nucl. Chem.* **263**, 355–360. (doi:10.1007/s10967-005-0062-9)
26. Owens SA. 2013 Advances in measurements of particle cycling and fluxes in the ocean. PhD Thesis. Woods hole, MA, Massachusetts Institute of Technology and Woods Hole Oceanographic Institution.
27. Stukel MR, Asher E, Couto N, Schofield O, Strebels S, Tortell P, Ducklow HW. 2015 The imbalance of new and export production in the western Antarctic Peninsula, a potentially ‘leaky’ ecosystem. *Glob. Biogeochem. Cycles* **29**, 1400–1420. (doi:10.1002/2015GB005211)
28. Eveleth R, Cassar N, Sherrell RM, Ducklow H, Meredith MP, Venables HJ, Lin Y, Li Z. 2017 Ice melt influence on summertime net community production along the Western Antarctic Peninsula. *Deep Sea Res. II* **139**, 89–102. (doi:10.1016/j.dsr2.2016.07.016)
29. Cassar N, Barnett BA, Bender ML, Kaiser J, Hamme RC, Tilbrook B. 2009 Continuous high-frequency dissolved O<sub>2</sub>/Ar measurements by equilibrator inlet mass spectrometry. *Anal. Chem.* **81**, 1855–1864. (doi:10.1021/ac802300u)
30. Schofield O *et al.* 2017 Decadal variability in coastal phytoplankton community composition in a changing West Antarctic Peninsula. *Deep Sea Res. I* **124**, 42–54. (doi:10.1016/j.dsr.2017.04.014)
31. Kim H, Doney SC, Iannuzzi RA, Meredith MP, Martinson DG, Ducklow HW. 2016 Climate forcing for dynamics of dissolved inorganic nutrients at Palmer Station, Antarctica: an interdecadal (1993–2013) analysis. *J. Geophys. Res. Biogeosci.* **121**, 2369–2389. (doi:10.1002/2015JG003311)
32. Ducklow HW, Erickson M, Kelly J, Smith RC, Stammerjohn SE, Vernet M, Karl DM. 2008 Particle export from the upper ocean over the continental shelf of the west Antarctic Peninsula: a long-term record, 1992–2006. *Deep Sea Res. II* **55**, 2118–2131. (doi:10.1016/j.dsr2.2008.04.028)
33. Chance R, Baker AR, Carpenter L, Jickells TD. 2014 The distribution of iodide at the sea surface. **16**, 1841–1859. (doi:10.1039/c4em00139g)
34. Campos MLAM, Farrenkopf AM, Jickells TD, Luther GW. 1996 A comparison of dissolved iodine cycling at the Bermuda Atlantic Time-series Station and Hawaii Ocean Time-series Station. II. *Top. Stud. Oceanogr.* **43**, 455–466. (doi:10.1016/0967-0645(95)00100-X)

35. Tian RC, Marty JC, Nicolas E, Chiavérini J, Ruiz-Ping D, Pizay MD. 1996 Iodine speciation: a potential indicator to evaluate new production versus regenerated production. *43*, 723–738. (doi:10.1016/0967-0637(96)00023-4)
36. Wong GTF. 2001 Coupling iodine speciation to primary, regenerated or ‘new’ production: a re-evaluation. *48*, 1459–1476. (doi:10.1016/S0967-0637(00)00097-2)
37. Martin P *et al.* 2013 Iron fertilization enhanced net community production but not downward particle flux during the Southern Ocean iron fertilization experiment LOHAFEX. *Glob. Biogeochem. Cycles* **27**, 871–881. (doi:10.1002/gbc.20077)
38. Vernet M, Martinson D, Iannuzzi R, Stammerjohn S, Kozłowski W, Sines K, Smith R, Garibotti I. 2008 Primary production within the sea-ice zone west of the Antarctic Peninsula: I—sea ice, summer mixed layer, and irradiance. *Deep Sea Res. II* **55**, 2068–2085. (doi:10.1016/j.dsr2.2008.05.021)
39. Jennings JC, Gordon LI, Nelson DM. 1984 Nutrient depletion indicates high primary productivity in the Weddell Sea. *Nature* **309**, 51–54. (doi:10.1038/309051a0)
40. Lance VP, Strutton PG, Vaillancourt RD, Hargreaves BR, Zhang J.-Z, Marra J. 2012 Primary productivity, new productivity, and their relation to carbon flux during two Southern Ocean gas exchange tracer experiments. *J. Geophys. Res. Oceans* **117**, C00F14. (doi:10.1029/2011JC007687)
41. Bowman J, Kavanaugh MT, Doney SC, Ducklow HW. In press. Recurrent seascape units identify key ecological processes along the western Antarctic Peninsula. *Glob. Change Biol.*
42. Stukel MR, Ducklow HW. 2017 Stirring up the biological pump: vertical mixing and carbon export in the Southern Ocean. *Glob. Biogeochem. Cycles* **31**, 1420–1434. (doi:10.1002/2017GB005652)
43. Stukel M, Benitez-Nelson C, Decima M, Taylor A, Buchwald C, Landry M. 2016 The biological pump in the Costa Rica Dome: an open-ocean upwelling system with high new production and low export. *J. Plankton Res.* **38**, 348–365. (doi:10.1093/plankt/fbv097)
44. Weston K, Jickells TD, Carson DS, Clarke A, Meredith MP, Brandon MA, Wallace MI, Ussher SJ, Hendry KR. 2013 Primary production export flux in Marguerite Bay (Antarctic Peninsula): Linking upper water-column production to sediment trap flux. *Deep Sea Res. I* **75**, 52–66. (doi:10.1016/j.dsr.2013.02.001)
45. Sambrotto RN, Burdloff D, McKee K. 2016 Spatial and year-to-year patterns in new and primary productivity in sea ice melt regions of the eastern Bering Sea. *Deep Sea Res. II* **134**, 86–99. (doi:10.1016/j.dsr2.2015.07.011)
46. Huang K, Ducklow H, Vernet M, Cassar N, Bender ML. 2012 Export production and its regulating factors in the West Antarctica Peninsula region of the Southern Ocean. *Glob. Biogeochem. Cycles* **26**, GB2005. (doi:10.1029/2010gb004028)
47. Buesseler KO, McDonnell AMP, Schofield OME, Steinberg DK, Ducklow HW. 2010 High particle export over the continental shelf of the west Antarctic Peninsula. *Geophys. Res. Lett.* **37**, 1–5. (doi:10.1029/2010GL045448)
48. Sherrell RM, Annett AL, Fitzsimmons JN, Rocanova VJ, Meredith MP. 2018 A ‘shallow bathtub ring’ of local sedimentary iron input maintains the Palmer Deep biological hotspot on the West Antarctic Peninsula shelf. *Phil. Trans. R. Soc. A* **376**, 20170171. (doi:10.1098/rsta.2017.0171)
49. Annett AL, Fitzsimmons JN, Seguret MJM, Lagerstrom M, Meredith MP, Schofield O, Sherrell RM. 2017 Controls on dissolved and particulate iron distributions in surface waters of the Western Antarctic Peninsula shelf. *Mar. Chem.* **196**, 81–97. (doi:10.1016/j.marchem.2017.06.004)
50. Sabine C, Feely R, Wanninkhof R, Dickson A, Millero F, Hansell D, Swift J, McNichol A, Key R. 2012 *Carbon dioxide, hydrographic, and chemical data obtained during the R/V nathaniel B. Palmer cruise in the Southern Ocean on CLIVAR repeat hydrography section S04P.* (ed. C. D. I. A. Center). Oak Ridge, TN: Oak Ridge National Laboratory, US Department of Energy.
51. Bodungen BV, Smetacek V, Tilzer MM, Zeitzschel B. 1986 Primary production and sedimentation during spring in the Antarctic Peninsula region. *Deep-Sea Research A* **33**, 177–194. (doi:10.1016/0198-0149(86)90117-2)
52. Tortell PD *et al.* 2014 Metabolic balance of coastal Antarctic waters revealed by autonomous pCO<sub>2</sub> and ΔO<sub>2</sub>/Ar measurements. *Geophys. Res. Lett.* **41**, GL061266. (doi:10.1002/2014GL061266)